

A BROADBAND TRANSVERSE KICKER PROTOTYPE FOR INTRA-BUNCH FEEDBACK IN THE CERN SPS

M. Wendt*, S. J. Calvo, W. Höfle, O. R. Jones, E. Montesinos, I. A. Romero
CERN, Geneva, Switzerland

Abstract

A transverse intra-bunch feedback system is currently under study at CERN for the SPS, to mitigate beam instabilities caused by electron clouds and coupled transverse modes (TMCI). This feedback system is designed for a bandwidth of 1 GHz, and based on a digital feedback controller and broadband power amplifiers. For the kicker, a periodic, quasi-TEM slotted transmission-line structure is foreseen which promises to meet the bandwidth requirements. This paper discusses the electromagnetic design and the mechanical implementation of a prototype kicker, demonstrating its performance and limitations based on numerical simulations.

INTRODUCTION

In frame of the LHC Injector Upgrade (LIU) project [1] at CERN, a transverse, intra-bunch feedback (FB) system is studied for use at the SPS, to mitigate high intensity instability effects caused by electron clouds or coupled transverse modes. The beams in the SPS are prepared for LHC physics runs in trains with 25 ns spaced bunches, and accelerated from an energy of 26 GeV/c at the injection, to 450 GeV/c at extraction. The bunches will have an intensity up to $3 \cdot 10^{11}$ protons with a length ranging from 1 – 3 ns (4σ).

To effectively fight intra-bunch instabilities, these beam parameters require a minimum bandwidth of DC – 1 GHz for the feedback system. A test installation at the SPS is based on a digital FB controller operating at a 4 GSPS data acquisition rate and broadband power amplifiers, both of which meet this bandwidth requirement [2]. For the kicker, different structures have been investigated [3, 4], such as dipole mode cavities, strip-line structures and, with most promising performance, a slotted waveguide coupler with inserted strip-line. The current test setup uses two strip-line kickers, however their bandwidth is limited to ~500 MHz. The design of a slotted waveguide, strip-line kicker structure based on the concept of L. Faltin [5] is therefore also being pursued.

Figure 1 shows the cross-section of the *Faltin*-type kicker structure, indicating some key parameters for the SPS prototype currently being manufactured. The mechanical dimensions have been fine-tuned based on a design report [3], published in the frame of the US LHC Accelerator Upgrade Program (LARP), which studied the parameter space of the slot dimensions, number of slots and pitch with respect to the transverse shunt impedance $R_{\perp} T^2$.

While the comprehensive report comes close to the optimum slot dimension, it misses a few aspects on the

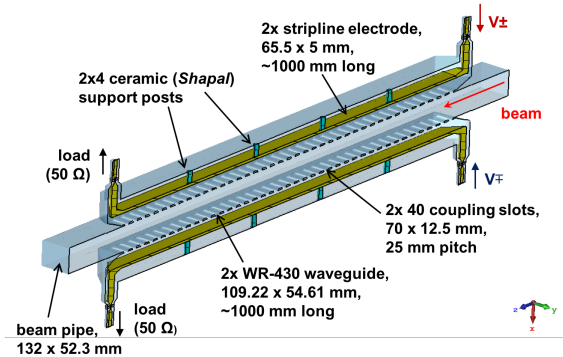


Figure 1: *Faltin*-type kicker structure.

impedance matching of the strip-lines, a transition with minimum reflections between strip-line and coaxial feedthrough, and some practical considerations such as isolated posts to keep the strip-line in place and also help to dissipate thermal power [6]. A series of numerical electro-magnetic simulations have been performed to include those aspects in the overall optimization procedure, also considering the necessary cooling of the strip-lines.

PRINCIPLE OF OPERATION

The fundamentals of an electromagnetic kicker, as well as the analogy to a beam pickup, is covered in [7]. Consider a charged particle e of constant velocity $v = ds/dt$ passing through a kicker device of length L . The electric E and magnetic B fields along the kicker path, driven by an external power source, will alter the momentum of the particle by

$$\Delta p = e \int_{t_a=0}^{t_b=L/v_z} (E + v \times B) dt \quad (1)$$

The transverse shunt impedance

$$R_{\perp} T^2 = \frac{V_{\perp}^2}{2P_{in}} \quad (2)$$

is the figure of merit, here for a kicker operating in the transverse plane, and relates the transverse beam voltage

$$V_{\perp}(\hat{x}, \hat{y}) = \int_0^L (E + v \times B)_{\perp} dz \quad (3)$$

to the applied input power P_{in} . The transit-time factor T corrects for the reduction of the maximum beam voltage due to the time it takes the particle to pass the time-varying fields of the kicker.

For the installation in the SPS the kicker will be arranged to operate vertically, as indicated in Fig. 1. However, for the numerical simulations the kicker was oriented differently.

* manfred.wendt@cern.ch

The x -coordinate therefore corresponds to the vertical axis in the SPS, and the y -coordinate to the horizontal. The z -coordinate is assigned to the longitudinal axis, i.e. in the beam direction. Under these assumptions eq. (3) simplifies to:

$$V_{\perp}(\hat{x}, \omega) = \int_0^L [E_x(z, \omega) - \beta c B_y(z, \omega)] e^{j \frac{\omega z}{\beta c}} dz \quad (4)$$

with the beam of velocity βc in the z -direction, $E_x(z, \omega)$, $B_y(z, \omega)$ expressed as frequency-domain complex field components on the $x = 0$, $y = 0$ symmetry axis, and $e^{j \frac{\omega z}{\beta c}}$ accounting for the transit time of the beam particles passing the kicker.

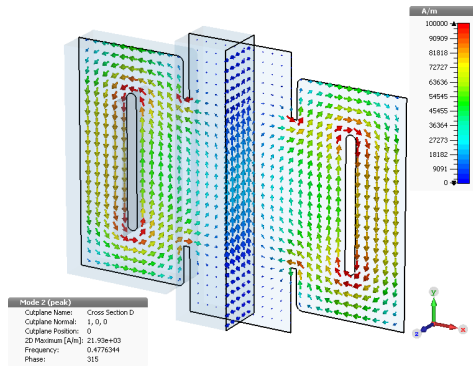


Figure 2: H-field of the Δ eigen-mode of a periodic *Falin*-type kicker cell.

As Fig. 1 indicates, the two symmetrically arranged slotted, strip-line loaded waveguides are fed on their upstream coaxial ports by differential (push-pull) drive signals from a broadband power amplifier. The kicker operates as a forward coupling, quasi-TEM traveling-wave periodic structure, acting on the TEM-field of the beam (for details see [5]). Figure 2 shows the H-field, which gives the major contribution to V_{\perp} at lower frequencies, of an eigen-mode analysis of one kicker cell. Here the phase advance of the E -field between the periodic boundaries in z -direction was set to 15° , which results in a Δ -mode frequency found at 477 MHz, represented by the purple colored point \blacktriangle in Fig. 3. A scan in steps of 2.5° , ranging from $2.5^\circ - 45^\circ$ of this boundary phase advance allows the phase velocity of the relevant Δ and Σ mode of the quasi-TEM traveling kicker field to be plotted against frequency. This phase velocity is $< c$, and as a consequence, the time slip Δt between beam and kicker field ultimately limits the maximum length of the periodic kicker structure. Here, for a kicker length of $L \approx 1$ m it is $\Delta t = 310$ ps for $f = 1.2$ GHz.

KICKER DESIGN

Design parameters have been analyzed and optimized in [3], with others, such as the beam pipe aperture and the design details of the high power coaxial feedthrough, a given. The cross-section dimensions of the waveguide were pragmatically chosen following the WR-430 waveguide standard. Figure 4 illustrates the mechanical details

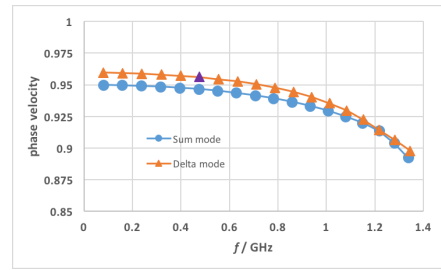


Figure 3: Phase velocity of the Δ and Σ eigen-modes.

of the kicker design. The entire 3-D kicker structure was entered in a parametrized format in the *CST Studio* electromagnetic (EM) simulation software to analyze the electromagnetic characteristics and performance of the kicker. The optimization was focused on the transition between stripline and coaxial feedthrough, minimizing the reflections, while including the ceramic posts along the stripline required to ensure mechanical stability and thermal power dissipation. The EM simulations also included the electrical effects of the materials chosen for the manufacturing, and evaluated the acceptable range of mechanical tolerances for a few critical details.

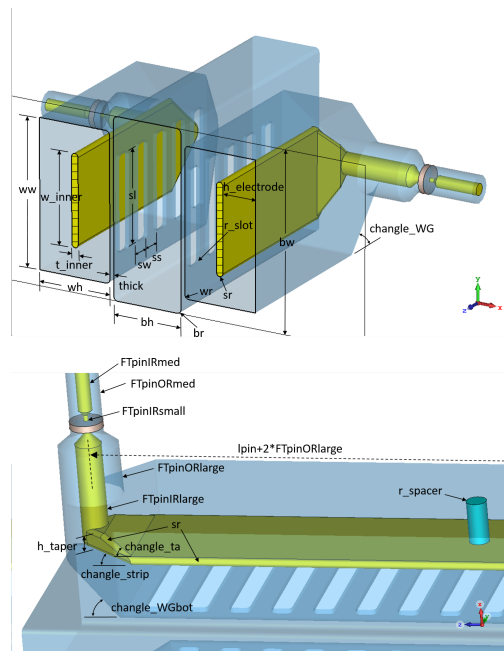


Figure 4: Design details of the kicker structure.

Transverse Shunt Impedance

Following Eq. (4), the $E_x(z, \omega)$ and $H_y(z, \omega)$ field components on the beam axis ($x = 0$, $y = 0$), i. e. the beam axis, of an EM simulation of a quarter of the kicker structure, applying symmetry boundaries with an electric wall in the yz -plane and a magnetic wall in the xz -plane, were recorded while applying a time-domain stimulus signal at the upstream port. A 100 MHz step interval was chosen to retrieve the complex, frequency domain E and H field components to compute the transverse shunt impedance based on eq. (1) and (4). The result presented in Fig. 5 indicate a

peak of the impedance at ~ 1.1 GHz, which corresponds to the TE_{01} waveguide cutoff frequency of the beam pipe.

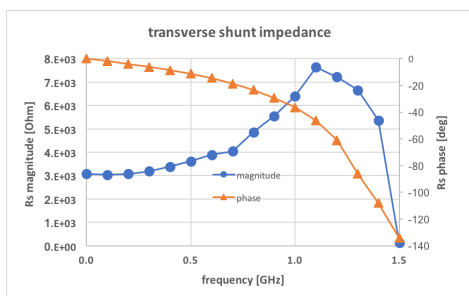


Figure 5: Design details of the kicker structure.

Impedance Matching

Figure 6 illustrates the impedance matching optimization of the stripline and the transition to the coaxial feedthrough, taking the four posts made out of machinable AIN ceramics (*Shapal*) into account. The coupling between the two opposite striplines is negligible, therefore particularities of the matching of even and odd mode impedances do not need to be addressed.

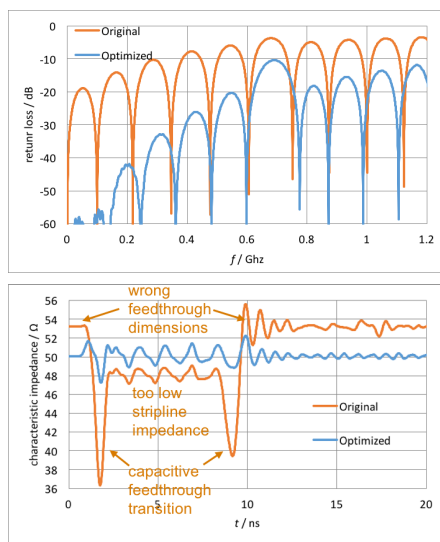


Figure 6: Return loss and time-domain reflectometry (TDR) before and after impedance matching of stripline and coaxial transition.

Beam Coupling Impedance

CST Studio wakefield analysis was performed to estimate the longitudinal wake potential $W_{\parallel}(z)$ and the related beam coupling impedance

$$Z_{\parallel}(\omega) = \frac{1}{\beta c} \int_{-\infty}^{\infty} W_{\parallel}(z) e^{-j\frac{\omega z}{\beta c}} dz \quad (5)$$

The result, presented in Fig. 7, shows no major resonance effects at frequencies below 1.5 GHz. Most of the beam coupled power losses will be coupled to the downstream ports and be absorbed in the load resistors. The longitudinal coupling impedance is therefore of minor concern.

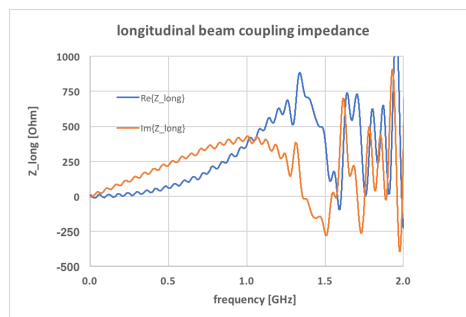


Figure 7: Real and imaginary part of the longitudinal coupling impedance.

PIC Simulation

The kicker performance was verified with a particle-in-cell (PIC) simulation. In the simulation, the kick response to a 50 ns duration, rectangular-shaped differential excitation signal on a quasi-DC beam passing the kicker on the z -axis was observed 1.8 m downstream of the kicker. The result, shown in Fig. 8, verifies the DC-coupling with no droop effects (left), and a fast rise time (right) of ~ 200 ps with some ringing, as expected from the $R_{\perp}T^2$ response shown in Fig. 5

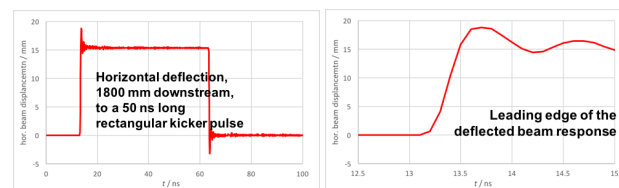


Figure 8: Beam displacement response of the quasi-DC beam, based on a PIC simulation.

CONCLUSIONS

A transverse, traveling-wave, *Falrin*-style kicker structure was analyzed and tuned to meet the requirements of the SPS intra-bunch feedback system. The EM simulations show no surprises, verifying a high bandwidth performance, which is also reflected by the smooth phase of the transverse voltage and the fast beam kick response demonstrated in the time-domain with a PIC simulation. Other parameters taken from the simulations, but not presented in this paper, such as field homogeneity and sensitivity to manufacturing tolerances, also proved to be satisfactory.

A prototype of the kicker is currently being manufactured, and will be installed in the SPS latest during the Long CERN Shutdown in 2019 – 2020. Further studies will be undertaken to scale the structure to achieve an even higher bandwidth.

ACKNOWLEDGEMENTS

The authors thank J. Cesaratto and S. Verdu for their many contributions in the initial design phase, and F. Caspers for the fruitful discussions.

REFERENCES

- [1] E. Shaposhnikova et al., “LHC Injectors Upgrade (LIU) Project at CERN”, Proc. of the IPAC2016, Busan, Korea, 2016, May 8 – 13, MOPOY059, pp. 992–995.
- [2] J. D. Fox et al., “Control of Intra-Bunch Vertical Instabilities at the SPS – Measurements and Technology Demonstration”, presented at IPAC’17, Copenhagen, Denmark, May 2017, paper TUPIK119, this conference.
- [3] J. M. Cesaratto et al., “SPS Wideband Transverse Feedback Kicker: Design Report”, SLAC, SLAC-R-1037, September 2013.
- [4] J. M. Cesaratto et al., “A Wideband Slotted Kicker Design for SPS Transverse Intra-Bunch Feedback”, Proc. of IPAC’13, Shanghai, China, 2013, paper WEPME016, p. 3073.
- [5] L. Faltin, “Slot-Type Pick-up and Kicker for stochastic Beam Cooling”, CERN, NIM 148 (1978), pp. 449–455.
- [6] T. Roggen et al., “Thermal Studies on the SPS Wideband Transverse Feedback Kicker”, CERN-ACC-NOTE-2016-0054, September 14, 2016.
- [7] D. A. Goldstein and G. R. Lambertson, “Dynamic Devices A Primer on Pickups and Kickers”, LBL-31664, University of California Berkeley, AIP Conferences Proceedings Series – Physics of Particle Accelerators, New York, NY, p. 192.